



## RESEARCH ARTICLE

## Estimation of lattice stress and strain in zinc ferrite nanoparticles by williamson-hall and size-strain plot methods

M. Augustin<sup>\*a</sup>, T. Balu<sup>b</sup>

<sup>a</sup> Department of Physics, St. Xavier's College (Autonomous), Palayamkottai– 627002, Tamil Nadu, India

<sup>b</sup> Department of Physics, Aditanar College of Arts & Science, Tiruchendur– 628 216, Tamil Nadu, India

Received 8 August 2015; Accepted 20 November 2015

Available online 10 December 2015

### Abstract

The Williamson-Hall (W-H) analysis and size-strain plot method (SSP) were used to study the lattice stress, strain and crystalline size of Zinc ferrite nanoparticles ( $\text{ZnFe}_2\text{O}_4$ ).  $\text{ZnFe}_2\text{O}_4$  nanoparticles were synthesized by chemical co-precipitation method and characterized by powder X-ray diffraction analysis (PXRD). The PXRD results revealed that the sample product was crystalline with mixed type spinel with cubic structure. The crystalline development in the  $\text{ZnFe}_2\text{O}_4$  was investigated by X-ray peak broadening. The physical parameters such as strain, stress and energy density values were calculated more precisely for all the reflection peaks of PXRD using the W-H plots and SSP method. The variation in particle size, lattice strain, stress and energy density calculated from W-H analysis and SSP method reveals that a non-uniform strains in the particles. This non-uniform strain was increased when the particles size were increased.

### Keywords

Nano particles  
X-ray techniques  
W-H analysis  
Co-precipitation

### Introduction

A perfect crystal would extend infinitely in all directions, so no crystals are perfect due to their finite size. This deviation from perfect crystallinity leads to a broadening of the diffraction peaks. The two main properties extracted from peak width analysis are the crystallite size and lattice strain. Crystallite size is a measure of the size of coherently diffracting domains.

The crystallite size of the particles is not generally the same as the particle size due to the formation of polycrystalline aggregates [1]. Lattice strain is a measure of the distribution of lattice constants arising from crystal imperfections, such as lattice dislocations. Other sources of strain include the grain boundary triple junction, contact or sinter stresses, stacking faults and coherency stresses [2]. Crystallite size and lattice strain affect the Bragg peak. Both these effects increase the peak width and intensity and shift the  $2\theta$  peak position accordingly. The effect of both uniform and non-uniform strain, on the direction of X-ray reflection is illustrated in Fig 1. A portion of an unstrained grain appears in

\*Corresponding author Tel. +919965424198  
E-mail : augustinbeny@gmail.com

panel (a) on the left, and the set of transverse reflecting planes shown has a uniform equilibrium spacing  $d$ . The diffraction line from these planes appears on the right. If a uniform tensile strain is applied to a grain at right angles to the reflecting planes, their spacing becomes larger than  $d$  and the corresponding diffraction line shifts to lower angles but does not otherwise change, as shown in panel (b). This line shift is the basis of the X-ray method for the measurement of macro stress. In (c) the grain is bent and the strain is non-uniform, on the top (tension) side the plane spacing exceeds  $d$ , whereas on the bottom (compression) side it is less than  $d$ , and somewhere in between it equals  $d_0$  [3].

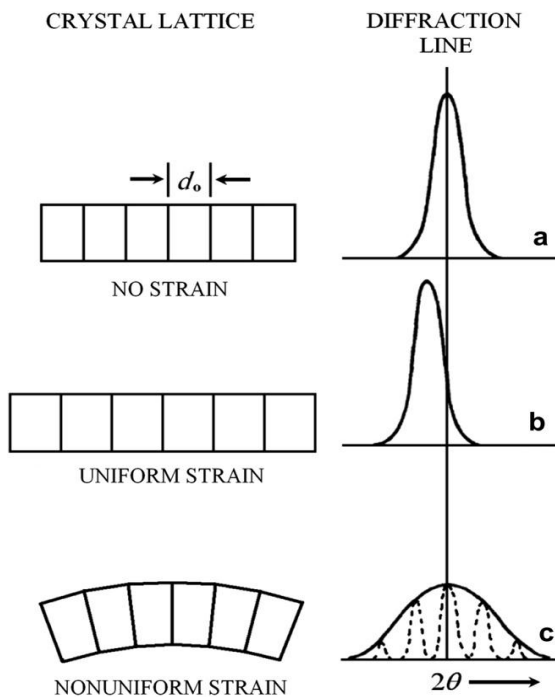


**Fig 1** (a) uniform strain (b) non-uniform strain (c) non-uniform strain affect the peak broadening.

However, the peak width derived from crystallite size varies as  $1/\cos\theta$ , whereas strain varies as  $\tan\theta$ . This difference in behavior as a function of  $2\theta$  enables one to discriminate between the size and strain effects on peak broadening. The Bragg width contribution from crystallite size is inversely proportional to the crystallite size [4]. X-ray profile analysis is a simple and powerful tool to estimate the crystallite size and lattice strain [5]. Among the available methods to estimate the crystallite size and lattice strain are the pseudo-Voigt function, Rietveld refinement, and Warren-Averbach analysis [6-8]. Williamson-Hall (W-H) analysis is a simplified integral breadth method where both size-induced and strain-induced broadening are deconvoluted by considering the peak width as a function of  $2\theta$  [9].

In this study, a chemical co-precipitate method was used to prepare Zinc ferrite nanoparticles. The strain due to lattice deformation associated with the  $\text{ZnFe}_2\text{O}_4$  nanoparticles annealed at  $800^\circ\text{C}$  was estimated by a modified form of W-H, namely uniform deformation model (UDM), uniform stress deformation model (USDM), uniform deformation energy-density model (UEDM) and the size-strain plot method (SSP) provide information on the stress-strain relation and the strain ( $\epsilon$ ) as a function of energy density ( $u$ ).

## Experimental

In the co-precipitation method, an aqueous solution of Zinc chloride and aqueous solution of ferric chloride was prepared with Fe-to-Zn mole ratio of 2:1. An aqueous solution of sodium hydroxide was used as the precipitant agent. The desired amount of aqueous solution of Zinc chloride and ferric chloride were taken and subjected to stirring using a magnetic stirrer for half an hour. Under stirring, the aqueous solution of sodium hydroxide was added drop wise to the mixed solution until a  $\text{pH} = 11.5$  was reached. The liquid precipitate was then brought to reaction temperature of  $80^\circ\text{C}$  and stirred for 1 h. The product was then cooled to room temperature. The precipitates were filtered and washed several times with deionised water. Finally, the precipitated powders were dried overnight using an oven at  $80^\circ\text{C}$  in order to remove excess water. The resulting material was annealed  $800^\circ\text{C}$  for 5 h [10].

## Results and discussion

The XRD pattern of the prepared sample was shown in **Fig 2**. The entire detectable peak indexed with the standard reference data (JCPDS: 89-7412). It was clearly seen that the reflection peaks became sharper indicating the enhancement of crystallinity.

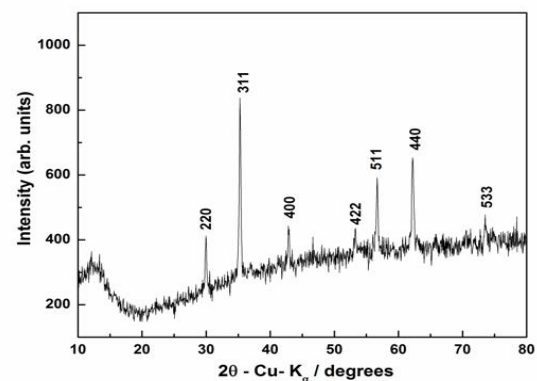


**Fig 2** XRD pattern of  $\text{ZnFe}_2\text{O}_4$  nanoparticles annealed at  $800^\circ\text{C}$  for 5 hrs

## Particle size and strain

XRD can be utilized to evaluate peak broadening with crystallite size and lattice strain due to dislocation [11]. The particle size of  $\text{ZnFe}_2\text{O}_4$  was determined by the X-ray line broadening method using the Debye-Scherrer equation

$$D = K\lambda/\beta_D \cos\theta \quad (1)$$

Where  $D$  is the particle size (nm),  $\lambda$  is the wavelength ( $\text{\AA}$ ),  $K$  is a constant (0.9),  $\beta_D$  is the peak width at half-maximum intensity and  $\theta$  is the peak position. The breadth of the Bragg peak is a combination of both instrument and sample dependent effects. To decouple these contributions, it is necessary to collect a diffraction pattern from the line broadening of a standard material such as silicon to determine the instrumental broadening. The instrument-corrected broadening [12]  $\beta_D$  corresponding to the diffraction peak of  $\text{ZnFe}_2\text{O}_4$  was estimated using the relation:

$$\beta_D = [(\beta^2)_{\text{measured}} - (\beta^2)_{\text{instrumental}}]^{1/2} \quad (2)$$

## Williamson-Hall methods

The Strain induced in powders due to crystal imperfections and distortion was calculated using the formula

$$\varepsilon = \beta_s/4\tan\theta \quad (3)$$

From equations (1) & (3) it is confirmed that peak width varies for crystallite size as  $1/\cos\theta$  and strain as  $\tan\theta$ . This fundamental difference allows that size and strain broadening are additive components of the total integral breadth of a Bragg peak [13].

$$\beta_{hkl} = \beta_s + \beta_D \quad (4)$$

$$\beta_{hkl} = (4\varepsilon\tan\theta) + (K\lambda/D \cos\theta) \quad (5)$$

Rearranging Eq. (5) gives

$$\beta_{hkl}\cos\theta = (K\lambda/D) + (4\varepsilon\sin\theta) \quad (6)$$

A plot is drawn (**Fig 3**) with  $4\sin\theta$  along the x-axis and  $\beta_{hkl}\cos\theta$  along the y-axis. From the linear fit to the data, the crystalline size was estimated from the y-intercept, and strain  $\varepsilon$ , from the slope of the fit. Eq. (6) represents the UDM, where the strain was assumed to be uniform in all crystallographic directions, thus considering the isotropic nature of the crystal, where the material properties are independent of the direction along which they are measured.

A generalized Hooke's law refers, linear proportionality between the stress and strain as given by  $\sigma = Y\varepsilon$ , where  $\sigma$

is the stress and  $Y$  is the Young's modulus. Applying the Hooke's law approximation to Eq. (6) yields

$$\beta_{hkl}\cos\theta = (K\lambda/D) + (4\sigma\sin\theta/Y_{hkl}) \quad (7)$$

The uniform stress can be calculated from the slope line plotted between  $4\sin\theta/Y_{hkl}$  and  $\beta_{hkl}\cos\theta$ , and crystallite size from the intercept as shown in **Fig 4**. Eq. (7) represents USDM and strain can be measured

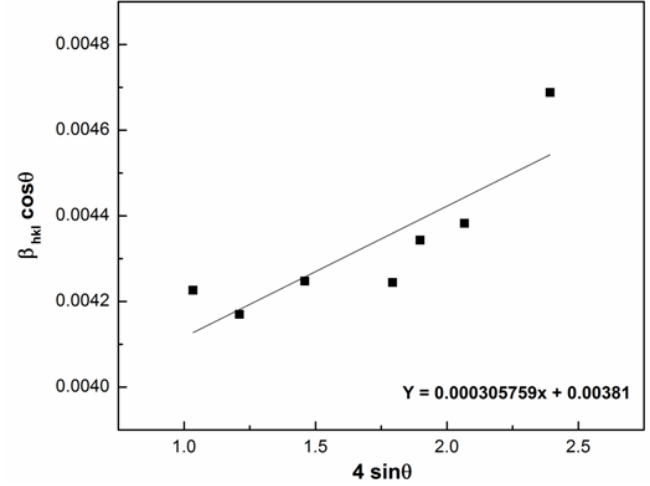


**Fig 3** Uniform deformation model (UDM) plot.

if  $Y_{hkl}$  of cubic  $\text{ZnFe}_2\text{O}_4$  nanoparticles is known. For samples with a cubic crystal phase,  $Y_{hkl}$  is related to their elastic compliances  $S_{ij}$  as

$$1/Y_{hkl} = S_{11} - 2[(S_{11} - S_{12}) - \frac{1}{2}S_{44}](l^2m^2 + m^2n^2 + n^2l^2) \quad (8)$$

Where  $S_{11}$ ,  $S_{12}$ ,  $S_{44}$  are the elastic compliances of  $\text{ZnFe}_2\text{O}_4$  nanoparticles and  $l$ ,  $m$ ,  $n$  are the cosines of the angles between the direction to which  $Y$  is referred and the crystal axes [14].  $S_{11}$ ,  $S_{12}$ ,  $S_{44}$  are related to their elastic stiffness as follows

$$C_{14} = 1/S_{44}, \quad C_{11} - C_{12} = (S_{11} - S_{12})^{-1}, \quad C_{11} + 2C_{12} = (S_{11} + 2S_{12})^{-1} \quad (9)$$

The values of elastic stiffness  $C_{11}$ ,  $C_{12}$ ,  $C_{14}$  for spinel ferrite are 275 GPa, 104 GPa, 95.5 GPa respectively [15].

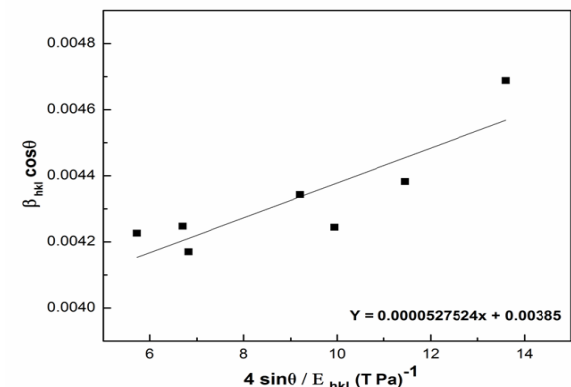


**Fig 4** Uniform stress deformation model (USDM) plot.

In Eq. (7), the assumption of homogeneity and isotropy is not justified. Moreover, the constants of proportionality associated with the stress-strain relation are no longer independent when the strain energy density  $u$  is considered. According to Hooke's law, the energy density as a function of strain and calculated from

$$u = (\varepsilon^2 Y_{hkl})/2 \quad (10)$$

Eq. (7) modified as

$$\beta_{hkl} \cos \theta = (K\lambda/D) + [4 \sin \theta (2u/Y_{hkl})^{1/2}] \quad (11)$$

Plot of  $\beta_{hkl} \cos \theta$  versus  $4 \sin \theta (2u/Y_{hkl})^{1/2}$  was constructed and the data fitted to line. The anisotropic energy density was estimated from the slope and crystallite size from the y-intercept. Eq. (11) represents UDEM and it is shown in **Fig 5**. The estimated values of lattice strain, stress, energy density and particle size were in **Table 1**.

### Size-Strain Plot method

In isotropic line broadening, a better evaluation of the size-strain parameters can be obtained by considering an average "size-strain plot", which has the advantage that less weight is given to data from reflections at high angles. In this approximation, it is assumed that the "crystallite size" profile is described by a Lorentzian function and the "strain profile" by a Gaussian function [16]. Accordingly, we have

$$(d_{hkl} \beta_{hkl} \cos \theta)^2 = K(d_{hkl}^2 \beta_{hkl} \cos \theta)/D + (\varepsilon/2)^2 \quad (12)$$

Where  $K$  is a constant equal to  $4/3$  for spherical particles and  $d$  is the lattice parameter.  $(d_{hkl} \beta_{hkl} \cos \theta)^2$  is plotted with respect to  $(d_{hkl}^2 \beta_{hkl} \cos \theta)$  and it is shown in **Fig 6**. The particle size is determined from the slope of the linearly fitted data and root of the y-intercept gives strain.

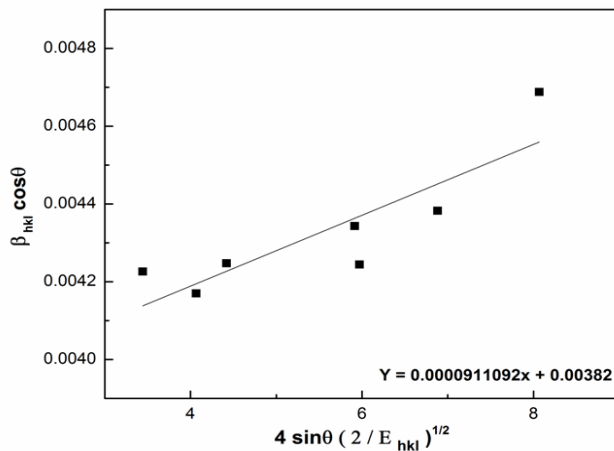


**Fig 5** Uniform deformation energy density model (UDEM) plot.

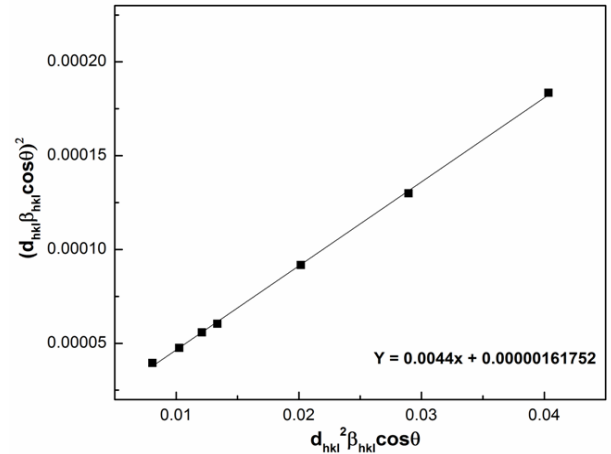


**Fig 6** Size-strain plot (SSP).

**Table 1** Geometric parameters of  $\text{ZnFe}_2\text{O}_4$  nanoparticles calcinated at  $800^\circ\text{C}$  for 5 h

Scherrer formula	Williamson-Hall method							
	UDM		USDM			UEDM		
D (avg) (nm)	D (nm)	$\varepsilon \times 10^{-4}$ (no unit)	D (nm)	$\varepsilon \times 10^{-4}$ (no unit)	$\sigma$ (MPa)	D (nm)	$\varepsilon \times 10^{-4}$ (no unit)	$\Sigma$ (MPa)
32.07	36.39	3.06	36.01	2.799	52.75	36.29	2.968	55.93

### Conclusions

$\text{ZnFe}_2\text{O}_4$  nanoparticles were synthesized by co-precipitation process and characterized by PXRD. The PXRD indicated that  $\text{ZnFe}_2\text{O}_4$  nanoparticles were crystalline with mixed type spinel with cubic structure. The line broadening of  $\text{ZnFe}_2\text{O}_4$  nanoparticles was due to the small crystallite size and lattice strain. This broadening was analyzed by the Scherrer formula, modified forms of W-H analysis and SSP method. From the results, it was observed that the values of crystallite size, lattice strain, stress and energy density calculated from the W-H analysis are slightly deviated with the SSP method. The crystallite size calculated from Scherrer formula also differs from the results of W-H method and SSP method. This variation in particle size, lattice strain, stress and energy density reveals that a non-uniform strains in the particles. This non-uniform strain was increased when the particles size was increased.

## Acknowledgments

The authors would like to thank Mr. Sridharan, Bharathiyar University, Coimbatore-641046, India for PXRD studies.

## References

- [1] K. Ramakanth, *Basic of Diffraction and its Application*, I. K. Inter. Pub. House Pvt. Ltd, New Delhi, (2007).
- [2] J. Zhang, Y. Zhang, K.W. Xu, V. Ji, *Solid State Commun.*, 139, (2006), 87.
- [3] N.S. Ramgir, Y.K. Hwang, I.S. Mulla, J.S. Chang, *Solid State Sci.*, 8, (2006), 359.
- [4] V.K. Pecharsky, P.Y. Zavalij, *Fundamentals of Powder Diffraction and Structural Characterization of Materials*, Springer, New York, (2003).
- [5] Cullity B D, Stock S R, *Elements of X-ray diffraction*, 3rd ed. Prentice Hall Pub., India, (2001).
- [6] H.M. Rietveld, *Acta Crystall.*, 22, (1976), 151.
- [7] D. Balzar, H. Ledbetter, *J. Appl. Crystall.*, 26, (1993), 97.
- [8] B.E. Warren, B.L Averbach, *J. Appl. Phys.*, 21, (1950), 595.
- [9] C. Suryanarayana, M.G. Norton, *X-ray Diffraction: A Practical Approach*, Springer, New York, (1998).
- [10] J.P. Jolivet, C. Chaneac, E. Tronc, *Chem. Commun.*, 5, (2004), 481.
- [11] R. Yogamalar, R. Srinivasan, A. Vinu, K. Ariga, A.C. Bose, *Solid State Commun.*, 149, (2009), 1919.
- [12] K.D. Rogers, P. Daniels, *Biomaterials*, 23, (2002), 2577.
- [13] M. Birkholz, *Thin Film Analysis by X-ray Scattering*, Wiley-VCH Verlag GmbH and Co. KGaA, Weinheim, (2006).
- [14] E.H.F. Date, K.W. Andrews, *J. Phys. D. Appl. Phys.* 2, (1969), 1373.
- [15] R.F.S Hearmon, *The elastic constants of crystals and other anisotropic materials*, in *Landolt-Bornstein Tables*, 111/18, 1-154, edited by K. H. Hellwege A.M. Hellwege, Springer-Verlag, Berlin, 559, (1984).
- [16] M.A. Tagliente, M. Massaro, *Nucl. Instrum Methods Phys. Res. B*, 266, (2008), 1055.